Curvature of the freeze-out line in heavy ion collisions

A. Bazavov,[1] H.-T. Ding,[2] P. Hegde,[2] O. Kaczmarek,[3] F. Karsch,[3,4] E. Laermann,[3] Swagato Mukherjee,[4] H. Ohno,[4,5]
P. Petreczky,[4] C. Schmidt,[3] S. Sharma,[4] W. Soeldner,[6] and M. Wagner[7]

[1]*Department of Physics and Astronomy, University of Iowa, Iowa City, Iowa 52240, USA*
[2]*Key Laboratory of Quark & Lepton Physics (MOE) and Institute of Particle Physics,*
Central China Normal University, Wuhan 430079, China
[3]*Fakultät für Physik, Universität Bielefeld, D-33615 Bielefeld, Germany*
[4]*Physics Department, Brookhaven National Laboratory, Upton, New York 11973, USA*
[5]*Center for Computational Sciences, University of Tsukuba, Tsukuba, Ibaraki 305-8577, Japan*
[6]*Institut für Theoretische Physik, Universität Regensburg, D-93040 Regensburg, Germany*
[7]*Physics Department, Indiana University, Bloomington, Indiana 47405, USA*

We calculate the mean and variance of net-baryon number and net-electric charge distributions from quantum chromodynamics (QCD) using a next-to-leading order Taylor expansion in terms of temperature and chemical potentials. We compare these expansions with experimental data from STAR and PHENIX, determine the freeze-out temperature in the limit of vanishing baryon chemical potential, and, for the first time, constrain the curvature of the freeze-out line through a direct comparison between experimental data on net-charge fluctuations and a QCD calculation. We obtain a bound on the curvature coefficient, $\kappa_2^f < 0.011$, that is compatible with lattice QCD results on the curvature of the QCD transition line.

I. INTRODUCTION

Heavy ion collisions at varying beam energies are performed at the Relativistic Heavy Ion Collider (RHIC) with the goal to probe properties of strong-interaction matter at different temperatures and baryon chemical potentials. This beam energy scan program aims to explore physics in the vicinity of the pseudocritical line of the transition from hadronic matter to the quark-gluon plasma. The hope is to find evidence for the existence of a critical point [1] in the phase diagram of strong-interaction matter that marks the end of a line of first-order phase transitions.

With decreasing beam energy, $\sqrt{s_{NN}}$, more baryons from the incident nuclei are stopped leading to an increase in the baryon number density and thus also to an increase of the baryon chemical potential in a central rapidity window. The dense matter created in these collisions is expected to reach local thermal equilibrium quickly. It subsequently expands and cools down. Eventually hadrons start to form again. This hadronization is characterized by a temperature (T) and baryon chemical potential (μ_B) that varies with $\sqrt{s_{NN}}$. Shortly thereafter inelastic interactions among the hadrons cease to occur and different particle species "freeze-out". This so-called chemical freeze-out is characterized by a set of freeze-out parameters, (T_f, μ_B^f). With varying $\sqrt{s_{NN}}$ they map out a line in the T-μ_B plane, called the freeze-out line, $T_f(\mu_B)$. An important question is how close the freeze-out line is to the pseudocritical line, $T_c(\mu_B)$ [2,3], characterizing the crossover transition of QCD. The proximity of both lines in the phase diagram is a prerequisite for being able to explore critical behavior in the

vicinity of a possibly existing critical point, by analyzing observables that can probe physics on the freeze-out line.

Unlike the crossover line, $T_c(\mu_B)$, for which the transition temperature at $\mu_B = 0$ [4,5] and the leading-order correction at small μ_B^2 [2,3] have been determined in lattice QCD calculations, the parametrization of the freeze-out line, $T_f(\mu_B)$, is not given in terms of fundamental parameters of QCD. The line characterizes the expanding medium formed in heavy ion collisions. Freeze-out parameters have been determined in a wide range of $\sqrt{s_{NN}}$ by comparing experimental data on particle yields with statistical hadronization models (HRG models). Parametrizations of the freeze-out line $T_f(\mu_B)$ have been extracted from such analyses [6,7]. Physically motivated ansätze, such as identifying $T_f(\mu_B)$ with a line of constant energy per particle [6], naturally lead to the expectation that $T_f(\mu_B)$ is a function of μ_B^2 that decreases with increasing μ_B. In fact, a simple ansatz [6],

$$T_f(\mu_B) = T_{f,0}(1 - \kappa_2^f \bar{\mu}_B^2 - \kappa_4^f \bar{\mu}_B^4), \qquad (1)$$

with $\bar{\mu}_B \equiv \mu_B/T_{f,0}$, provides a good parametrization in the entire energy range probed in heavy ion collisions. Using this ansatz for the comparison of HRG model calculations with experimental data obtained for a wide range of energies $\sqrt{s_{NN}}$ gave $\kappa_2^f = 0.023(3)$ [6] for the curvature coefficient. However, a recently performed refined hadronization model analysis suggests a weaker energy dependence of the freeze-out line [8]. Moreover, the attempt to capture more accurately the behavior of

freeze-out temperatures at large $\sqrt{s_{NN}}$, i.e., small μ_B, lead to a phenomenological parametrization [7] that does not even have a power-like dependence on μ_B, i.e., $T_f(\mu_B) - T_{f,0} \sim \exp(-a/\mu_B)$ which favors $\kappa_2^f \simeq 0$.

In this paper we improve over the current situation by outlining a procedure to determine the $\mathcal{O}(\mu_B^2)$ coefficient of the freeze-out line from measurements of the mean and variance of net-electric charge and net-proton number distributions and, for the first time, illustrate how this can be done by comparing experimental data obtained at large $\sqrt{s_{NN}}$ directly with a QCD calculation. This puts the determination of the curvatures of the freeze-out line on a par with that of the QCD transition line.

II. RATIO ON CHARGE FLUCTUATIONS ON THE FREEZE-OUT LINE

The mean, $M_X \equiv \chi_1^X(T,\mu)$, and variance, $\sigma_X^2 \equiv \chi_2^X(T,\mu)$, of net-electric charge ($X = Q$) and net-baryon number ($X = B$) distributions are obtained as functions of T and $\mu \equiv (\mu_B, \mu_Q, \mu_S)$ by taking derivatives of the QCD pressure with respect to $\hat{\mu}_X \equiv \mu_X/T$

$$\chi_n^X(T,\mu) = \frac{\partial^n P/T^4}{\partial \hat{\mu}_X^n}, \qquad X = B, Q, S. \qquad (2)$$

The ratios of mean and variance,

$$R_{12}^X(T,\mu) \equiv \frac{M_X}{\sigma_X^2} = \frac{\chi_1^X(T,\mu)}{\chi_2^X(T,\mu)}, \qquad (3)$$

can be analyzed in heavy ion experiments. Implementing the constraints $M_S = 0$ and $M_Q/M_B = r$, which are appropriate for the initial conditions met in such collisions, the ratios R_{12}^B and R_{12}^Q become functions of T and μ_B only and $\Sigma_r^{QB} \equiv R_{12}^Q/R_{12}^B = r\sigma_B^2/\sigma_Q^2$. In leading-order (LO) Taylor expansion Σ_r^{QB} is independent of $\hat{\mu}_B$, while the ratios R_{12}^B and R_{12}^Q depend linearly on $\hat{\mu}_B$, $R_{12}^X = R_{12}^{X,1}\hat{\mu}_B + \mathcal{O}(\hat{\mu}_B^3)$. They therefore provide mutually independent information that can be used to extract $T_f(\mu_B)$ up to $\mathcal{O}(\mu_B^2)$ [9].

In order to determine the freeze-out temperature at $\mu_B = 0$ and the curvature of the freeze-out line, we consider a next-to-leading order Taylor expansion of Σ_r^{QB} in terms of T and $\hat{\mu}_B$ around the point $(T_{f,0}, \mu_B = 0)$ with $\hat{\mu}_S$ and $\hat{\mu}_Q$ being implicit functions of T and $\hat{\mu}_B$. Using Eq. (1) as a parametrization of the freeze-out line, we find in next-to-leading order (NLO),

$$\Sigma_r^{QB} = \Sigma_r^{QB,0} + \left(\Sigma_r^{QB,2} - \kappa_2^f T_{f,0} \frac{d\Sigma_r^{QB,0}}{dT}\bigg|_{T_{f,0}} \right)\hat{\mu}_B^2. \qquad (4)$$

The LO expansion coefficient is easily related to the quadratic fluctuations of net-electric charge and net-baryon

number, $\Sigma_r^{QB,0} = r\chi_2^B(T)/\chi_2^Q(T)$ at zero $\hat{\mu}_B$. The NLO expansion coefficient $\Sigma_r^{QB,2}$ depends on fourth-order cumulants, which also can be calculated in a lattice QCD calculation at vanishing μ_B. An explicit expression for $\Sigma_r^{QB,2}$ will be given elsewhere [10].

In order to facilitate a comparison with the experimental data it is of advantage to eliminate $\hat{\mu}_B$ from Eq. (4) in favor of observables that are accessible to experiments and QCD calculations. For a consistent treatment of the NLO result, Eq. (4), it suffices to use the LO relation between $\hat{\mu}_B$ and the ratio R_{12}^B, i.e., $\hat{\mu}_B = R_{12}^B/R_{12}^{B,1}$. The LO expansion coefficient $R_{12}^{B,1}$ has been evaluated before and continuum extrapolated results for $m_l = m_s/20$ obtained with the highly improved staggered quark (HISQ) action have been shown in [11].

After replacing $\hat{\mu}_B$ in favor of R_{12}^B, the NLO Taylor expansion of Σ_r^{QB}, introduced in Eq. (4), becomes

$$\Sigma_r^{QB} = a_{12}(1 + c_{12}(R_{12}^B)^2) + \mathcal{O}((R_{12}^B)^4), \qquad (5)$$

where $a_{12}(T) \equiv \Sigma_r^{QB,0}$. The coefficient of the quadratic correction, c_{12}, depends on the parametrization of the freeze-out line and needs to be determined at $T_{f,0}$,

$$c_{12}(T_{f,0}, \kappa_2^f) = c_{12}^0(T_{f,0}) - \kappa_2^f D_{12}(T_{f,0}) \qquad (6)$$

with

$$c_{12}^0(T) = \left(\frac{1}{R_{12}^{B,1}}\right)^2 \frac{\Sigma_r^{QB,2}}{\Sigma_r^{QB,0}},$$

$$D_{12}(T) = \left(\frac{1}{R_{12}^{B,1}}\right)^2 T \frac{d \ln \Sigma_r^{QB,0}}{dT}. \qquad (7)$$

In Fig. 1 we show results for $\Sigma_r^{QB,0}$, $R_{12}^{B,1}$ and c_{12}^0 obtained in lattice QCD calculations with the $(2+1)$-flavor HISQ action [12] using a physical value of the strange quark mass and two sets of light quark masses, $m_l = m_s/20$, $m_s/27$, which in the continuum limit correspond to pion mass values, $m_\pi \simeq 160$ and 140 MeV, respectively. Here we used $r \simeq 0.4$ which is appropriate for describing colliding gold or lead nuclei. Further details on the simulation parameters can be found in [13]. We note that quark mass effects are small for the observables under consideration.

The continuum extrapolated results for $\Sigma_r^{QB,0}$ and $R_{12}^{B,1}$ in the left and middle panels of Fig. 1 were obtained by performing cubic spline fits to all $m_l = m_s/20$ data, with $1/N_\tau^2$ dependence for the spline coefficients and for the varying locations of three knots. These fits were performed over many bootstrap samples drawn from the Gaussian errors of data points and have been constrained to agree with HRG at $T = 130$ MeV within 10%. The final continuum results were obtained from mean values and errors
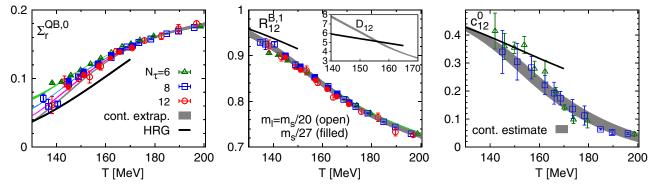
FIG. 1.   Temperature dependence of the LO expansion coefficients of the ratio Σ_r^{QB} (left) and R_{12}^B (middle) and the NLO coefficient c_{12}^0 (right) introduced in Eq. (7). The NLO coefficient D_{12} [Eq. (7)] is shown as an insertion in the middle panel. Shown are data from calculations with the HISQ action on lattices of size $N_\sigma^3 \times N_\tau$, with $N_\sigma = 4N_\tau$. Bands show continuum extrapolations for the LO observables and continuum estimates for the NLO observable c_{12}^0 (see text).

of these bootstrapped fit results weighted by the quality of the fits given by the Akaike information criteria. The continuum extrapolations are consistent with our earlier results [13]. However, statistical errors are reduced considerably.

The parameter D_{12} is obtained from the continuum extrapolated results for $R_{12}^{B,1}$ and $\Sigma_r^{QB,0}$. It is shown as an insertion in the middle panel of Fig. 1. The coefficient c_{12}^0 receives contributions from fourth-order cumulants and thus is more difficult to extract. At present we have calculated it for two lattice spacings and therefore only provide an estimate for its continuum limit. This is shown in the right panel of Fig. 1. For the continuum estimate of c_{12}^0 we followed an identical procedure of the cubic spline fits outlined above but with only two knots.

A determination of Σ_r^{QB} and R_{12}^B at large $\sqrt{s_{NN}}$ suffices to fix the freeze-out temperature $T_{f,0}$ and the quadratic correction c_{12}. Combining this with lattice QCD results on c_{12}^0 and D_{12} allows to extract the curvature, κ_2^f, of the freeze-out line. However, in heavy ion collisions Σ_r^{QB} and R_{12}^B are not directly accessible. Net-proton rather than net-baryon numbers, i.e., ratios like R_{12}^P and Σ_r^{QP} rather than R_{12}^B and Σ_r^{QB}, are measured. The STAR Collaboration obtained R_{12}^P in the transverse momentum interval $0.4 \text{ GeV} \leq p_t \leq p_t^{\max}$ with $p_t^{\max} = 0.8$ GeV (STAR0.8) [14]. The p_t range has recently been extended, and preliminary results up to $p_t^{\max} = 2.0$ GeV (STAR2.0) [15] have been presented. The ratio of net-electric charge fluctuations, R_{12}^Q, has been measured by STAR [16] and PHENIX [17] in the interval $p_t^{\min} \leq p_t \leq 2.0$ GeV with $p_t^{\min} = 0.2$ GeV and $p_t^{\min} = 0.3$ GeV [18], respectively. Figure 2 shows results for Σ_r^{QP} versus $(R_{12}^P)^2$. In the case of the PHENIX data for R_{12}^Q, we used the STAR2.0 data set to construct Σ_r^{QP}.

Before entering into details of the analysis of these data using lattice QCD calculations for R_{12}^B and R_{12}^Q, we

need to discuss systematic effects that arise in equilibrium thermodynamics [19] because net-proton rather than net-baryon numbers are measured in experiments and because only data from a limited region in momentum space are available. The influence of low and high momentum cuts on charge fluctuations has been analyzed in HRG models [22,23]. The most important effects arise from a nonzero $p_t^{\min}$ which most drastically influences the pion contributions to net-electric charge fluctuations.
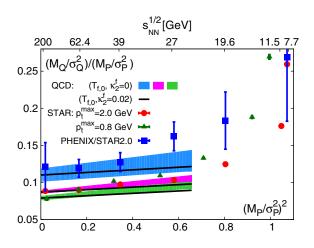

FIG. 2.   The ratio of ratios of mean and variance for net-electric charge and net-proton number fluctuations measured by the STAR and PHENIX Collaborations. For the STAR electric charge data [16], we show results obtained by normalizing with net-proton results from the published STAR0.8 data set [14] (triangles) as well as the preliminary STAR2.0 data set [15] (circles). The experimental data are compared to QCD predictions for two values of κ_2^f (see text). The electric charge results obtained by PHENIX [17] have been normalized by using the STAR2.0 data set on net-proton fluctuations (boxes). For orientation the upper x-axis shows $\sqrt{s_{NN}}$ energies of the RHIC beam energy scan with labels put at the values for $(M_P/\sigma_P)^2$ corresponding to the STAR2.0 data set. Errors on $(M_P/\sigma_P)^2$ are not visible as they are smaller than the size of the symbols.

Implementing the p_t-cuts STAR has used for protons and other charged particles [16] in a HRG model calculation suggests that R_{12}^Q is overestimated by about 5% while the larger $p_t^{\min} = 0.3$ GeV used by PHENIX [17] amounts to an increase of 20% [23]. This explains about 40% of the difference in R_{12}^Q seen by STAR and PHENIX. It is conceivable that the remainder arises from the small azimuthal coverage in the PHENIX experiment which further reduces the acceptance of charged particles [24]. In order to get better control over these effects a more detailed experimental study of systematics of arising from nonzero p_t cuts and cuts in the rapidity coverage will be needed.

With proton number not being a conserved quantity [21], the ratio R_{12}^P clearly has no meaning in the high temperature plasma phase of QCD. At chemical freeze-out, however, when inelastic interactions are no longer of relevance, the net-proton number may be considered to be a well-defined concept. Still R_{12}^P and R_{12}^B will differ in equilibrium thermodynamics. The difference can be estimated in a HRG model calculation where $R_{12}^P = \tanh(\hat{\mu}_B + \hat{\mu}_Q)$, independent of the value $\hat{\mu}_S$, while R_{12}^B explicitly depends on $\hat{\mu}_S$ [Eq. (3)]. For our NLO analysis of cumulant ratios it suffices to determine the LO relation between R_{12}^P and R_{12}^B. Using Taylor expansions for both, this obviously yields $R_{12}^B/R_{12}^P = R_{12}^{B,1}$, which is shown in the middle panel of Fig. 1.

The above discussion suggests that in the STAR measurements the systematic errors of R_{12}^Q and R_{12}^B are of similar magnitude and tend to cancel to a large extent in the ratio Σ_r^{QB}; i.e., the ratio Σ_r^{QP} indeed seems to be a good proxy for Σ_r^{QB} while for the PHENIX set-up it overestimates Σ_r^{QB} by at least 10%.

We have fitted the three data sets corresponding to the published STAR data (STAR0.8), the preliminary STAR data (STAR2.0) and the PHENIX data on net-charge fluctuations normalized to the STAR data on net-proton fluctuations (PHENIX/STAR2.0) using the ansatz given in Eq. (5). These data are shown in Fig. 2. For each of these three data sets two different fit ranges have been chosen, $R_{12}^P \leq 0.6$ and 0.8, which correspond to data taken at $\sqrt{s_{NN}} \geq 39$ GeV and 27 GeV, respectively. This determines the intercept a_{12} and the curvature parameter c_{12} given in Table I. Differences arising from the two fit ranges have been added as systematic error in the error analysis of a_{12} and c_{12}. From the intercept at $R_{12}^{P/B} = 0$ the freeze-out temperature $T_{f,0}$ is obtained. Once $T_{f,0}$ is fixed this way the NLO expansion coefficients c_{12}^0 and D_{12} are also fixed (see Table I) and we obtain QCD predictions for Σ_r^{QB} with κ_2^f as the sole free parameter. In Fig. 2 we show Σ_r^{QB} as a function of $(R_{12}^P)^2$ for $\kappa_2^f = 0$ (colored bands). Note that any value $\kappa_2^f > 0$ will result in a weaker dependence of Σ_r^{QB} on R_{12}^P.

TABLE I. Parameters of a quadratic fit to the STAR data on the ratio Σ_r^{QP} and the combination of PHENIX data on R_{12}^Q and STAR data on R_{12}^P. The third to fifth row give the freeze-out temperature $T_{f,0}$, c_{12}^0 and D_{12} at fixed $T_{f,0}$. The last row gives the curvature coefficients κ_2^f obtained from Eq. (6). In the fits none of the corrections discussed in the text have been taken into account.

	STAR0.8	STAR2.0	PHENIX/STAR2.0
a_{12}	0.079(3)	0.087(2)	0.110(9)
c_{12}	0.858(101)	0.329(74)	0.559(352)
$T_{f,0}$ [MeV]	145(2)	147(2)	155(4)
$c_{12}^0(T_{f,0})$	0.343(31)	0.326(32)	0.265(52)
$D_{12}(T_{f,0})$	7.04(44)	6.62(36)	5.27(78)
κ_2^f	−0.073(16)	−0.001(12)	−0.056(67)

As an illustration we also show the result for Σ_r^{QB} at $T_{f,0}$ and $\kappa_2^f = 0.02$. as black lines.

III. CURVATURE OF THE FREEZE-OUT LINE

We now can discuss constraints for the curvature coefficient κ_2^f resulting from the measured cumulant ratios Σ_r^{QB}. We consider the STAR data where cumulant ratios of net-electric charge as well as net-proton number fluctuations have been measured. As discussed earlier we consider Σ_r^{QP} to be a good approximation for the ratio Σ_r^{QB}. The difference between R_{12}^P and R_{12}^B can be corrected for by using the HRG model motivated correction, $R_{12}^P = R_{12}^B/R_{12}^{B,1}$. This is appropriate for our NLO approximation and simply amounts to a rescaling of the abscissa in Fig. 2. While the intercept a_{12} in quadratic fits is not influenced by such a rescaling, c_{12} increases by a factor $(R_{12}^{B,1})^{-2}$, i.e., by about 20% in the relevant temperature range. From Eq. (6) it is obvious that this will decrease the estimate for κ_2^f. Analyzing the uncorrected STAR data, thus, will put an upper bound on κ_2^f.

Results for c_{12} from quadratic fits to the two STAR data sets are given in Table I. We notice first that c_{12} extracted from the published STAR data [14,16] is about a factor of 2 larger than the lattice QCD result for $c_{12}^0(T_{f,0})$. Since D_{12} is positive, this corresponds to negative values for κ_2^f as observed also in a HRG model analysis [25], i.e., the STAR data on proton fluctuations taken in the range 0.4 GeV $\leq p_t \leq 0.8$ GeV [14] are only compatible with a negative curvature coefficient κ_2^f. However, the still preliminary STAR data taken in the larger p_t interval [15] have a much smaller slope which is consistent with $c_{12}^0(T_{f,0})$ within statistical errors. This gives an upper bound on the curvature of the freeze-out line,

$$\kappa_2^f < 0.011. \qquad (8)$$

Taking into account the HRG motivated correction for replacing R_{12}^P by R_{12}^B reduces κ_2^f and makes the estimate for the upper bound compatible with zero, $\kappa_2^f = -0.012(15)$ for the STAR2.0 data set; i.e., the existing data for Σ_r^{QP} favor a small or even vanishing curvature of the freeze-out line at large $\sqrt{s_{NN}}$ as it is the case for the phenomenological parametrization given in Ref. [7].

Let us finally compare the result obtained for κ_2^f with the curvature coefficient $\kappa_2^B > 0$ of the QCD transition line,

$$T_c(\mu_B) = T_{c,0}(1 - \kappa_2^B \hat{\mu}_B^2 + \mathcal{O}(\hat{\mu}_B^4)), \qquad (9)$$

where $T_{c,0}$ denotes the transition temperature at $\mu_B = 0$ [4,5]. The above bound on κ_2^f is consistent with determinations of κ_2^B based on expansions of $T_c(\mu_B)$ around $\mu_B = 0$ where the curvature coefficient is determined as a Taylor expansion coefficient evaluated at $\mu_B = 0$. This gave $\kappa_2^B \simeq 0.007$ [2,3], which is about a factor two smaller than recent results for κ_2^B [26–28] that are based on lattice QCD calculations performed with large nonzero imaginary chemical potentials, corresponding to $\mu_B/T_{c,0} \simeq (1-3)$. These calculations yield values $\kappa_2^B \simeq (0.015\text{–}0.02)$.

IV. CONCLUSIONS

We provided a framework that allows to determine the curvature of the freeze-out line through a direct comparison between experimental data for mean and variance of net-electric charge and net-proton number fluctuations with lattice QCD calculations of cumulant ratios. We found the curvature of the freeze-out line to be small. It is consistent with the curvature of the QCD crossover line. At least for beam energies $\sqrt{s_{NN}} \geq 27$ GeV, our study suggests that freeze-out happens close to the crossover transition line.

We have addressed some difficulties that arise when comparing lattice QCD calculations of conserved charge fluctuations with experimental data on cumulants of net-proton and net-charge fluctuations, although at present it is difficult to provide a complete quantitative approach for this. We have pointed out some obvious differences between net-proton and net-baryon number fluctuations that are present already in equilibrium thermodynamics. We also addressed the question on the influence of transverse

momentum cuts on the experimental data. Clearly control over these effects needs to be improved in future work. It also is known that cumulants of conserved charge fluctuations are sensitive to the width of the rapidity window covered by the experiments [29,30]. This dependence is more significant for net-electric charge fluctuations than for net-proton number fluctuations. Increasing the rapidity window will decrease σ_Q and thus will lead to an increase of Σ_r. This will lead to larger values for $T_{f,0}$. However, at present these effects are difficult to quantify.

Finally we note that throughout our analysis we assumed that the net-charge to net-baryon number ratio, r, is determined by the corresponding ratio present in the incident beams, $r \simeq 0.4$. This ratio clearly will fluctuate in a fixed acceptance range covered in an experiment and one may argue that this ratio also shifts towards the isospin symmetric limit $r = 0.5$ for high beam energies. Clearly, at present beam energies $r < 0.5$, as the net-charge expectation value would vanish in the isospin symmetric limit. In a more refined analysis one may, however, take into account effects arising from changes in the value of r which may also be beam energy dependent. In general, increasing r results in a decrease of $T_{f,0}$ and an increase of κ_2^f. Compared to other uncertainties, however, this effect is small. For the preliminary STAR data set (STAR2.0), we find, for instance, that using $r = 0.45$ decreases the $T_{f,0}$ by 3 MeV and shifts the curvature coefficient to a slightly positive value, $\kappa_2^f = 0.004$.

[1] M. Asakawa and K. Yazaki, Nucl. Phys. **A504**, 668 (1989); A. M. Halasz, A. D. Jackson, R. E. Shrock, M. A. Stephanov, and J. J. M. Verbaarschot, Phys. Rev. D **58**, 096007 (1998).

[2] O. Kaczmarek, F. Karsch, E. Laermann, C. Miao, S. Mukherjee, P. Petreczky, C. Schmidt, W. Soeldner, and W. Unger, Phys. Rev. D **83**, 014504 (2011).

[3] G. Endrodi, Z. Fodor, S. D. Katz, and K. K. Szabó, J. High Energy Phys. 04 (2011) 001.

[4] Y. Aoki, S. Borsányi, S. Dürr, Z. Fodor, S. D. Katz, S. Krieg, and K. Szabo, J. High Energy Phys. 06 (2009) 088.

[5] A. Bazavov et al., Phys. Rev. D **85**, 054503 (2012).

[6] J. Cleymans, H. Oeschler, K. Redlich, and S. Wheaton, Phys. Rev. C **73**, 034905 (2006).

[7] A. Andronic, P. Braun-Munzinger, and J. Stachel, Nucl. Phys. **A772**, 167 (2006).

[8] F. Becattini, M. Bleicher, T. Kollegger, T. Schuster, J. Steinheimer, and R. Stock, Phys. Rev. Lett. **111**, 082302 (2013).

[9] F. Karsch, Central Eur. J. Phys. **10**, 1234 (2012).

[10] Bielefeld-BNL-CCNU Collaboration (to be published).

[11] A. Bazavov *et al.*, Phys. Rev. Lett. **109**, 192302 (2012).

[12] E. Follana, Q. Mason, C. Davies, K. Hornbostel, G. P. Lepage, J. Shigemitsu, H. Trottier, and K. Wong (HPQCD Collaboration and UKQCD Collaboration), Phys. Rev. D **75**, 054502 (2007).

[13] A. Bazavov *et al.* (HotQCD Collaboration), Phys. Rev. D **86**, 034509 (2012).

[14] M. M. Aggarwal *et al.* (STAR Collaboration), Phys. Rev. Lett. **105**, 022302 (2010).

[15] X. Luo (STAR Collaboration), *Proc. Sci.*, CPOD2015 (2015) 019.

[16] L. Adamczyk *et al.* (STAR Collaboration), Phys. Rev. Lett. **113**, 092301 (2014).

[17] A. Adare *et al.* (PHENIX Collaboration), arXiv:1506.07834.

[18] In addition to this different coverage of the p_t range for charged particles, the measurements differ in the coverage of azimuthal angle. Furthermore, STAR has eliminated all protons and antiprotons with $p_t \leq 0.4$ GeV from their data sample.

[19] We refrain here from a discussion of possible nonequilibrium effects [20] or effects arising from additional inelastic scatterings after freeze-out [21]. This may play a role in the quantitative analysis of charge fluctuations, but goes beyond the equilibrium framework we try to establish here.

[20] S. Mukherjee, R. Venugopalan, and Y. Yin, Phys. Rev. C **92**, 034912 (2015).

[21] M. Kitazawa and M. Asakawa, Phys. Rev. C **85**, 021901 (2012).

[22] P. Garg, D. K. Mishra, P. K. Netrakanti, B. Mohanty, A. K. Mohanty, B. K. Singh, and N. Xu, Phys. Lett. B **726**, 691 (2013).

[23] F. Karsch, K. Morita, and K. Redlich, arXiv:1508.02614.

[24] A. Bzdak and V. Koch, Phys. Rev. C **86**, 044904 (2012).

[25] P. Alba, W. Alberico, R. Bellwied, M. Bluhm, V. M. Sarti, M. Nahrgang, and C. Ratti, Phys. Lett. B **738**, 305 (2014).

[26] C. Bonati, M. D'Elia, M. Mariti, M. Mesiti, F. Negro, and F. Sanfilippo, Phys. Rev. D **92**, 054503 (2015).

[27] R. Bellwied, S. Borsanyi, Z. Fodor, J. Günther, S. D. Katz, C. Ratti, and K. K. Szabo, Phys. Lett. B **751**, 559 (2015).

[28] P. Cea, L. Cosmai, and A. Papa, arXiv:1508.07599.

[29] B. Abelev *et al.* (ALICE Collaboration), Phys. Rev. Lett. **110**, 152301 (2013).

[30] M. Sakaida, M. Asakawa, and M. Kitazawa, Phys. Rev. C **90**, 064911 (2014).